

Transport and Deposition of Metabolically Active and Stationary Phase *Deinococcus radiodurans* in Unsaturated Porous Media

G. GARGIULO,^{*,†} S. A. BRADFORD,[‡]
J. ŠIMŮNEK,[§] P. USTOHAL,[†]
H. VEREECKEN,[†] AND E. KLUMPP[†]

Agrosphere (ICG-IV), Institute of Chemistry and Dynamics of the Geosphere (ICG), Forschungszentrum Jülich GmbH D-52425, Jülich, Germany, Salinity Laboratory, USDA-ARS, 450 West Big Springs Road, Riverside, California 92507-4617, and Department of Environmental Sciences, University of California, Riverside, California 92521

Bioremediation is a cost-efficient cleanup technique that involves the use of metabolically active bacteria to degrade recalcitrant pollutants. To further develop this technique it is important to understand the migration and deposition behavior of metabolically active bacteria in unsaturated soils. Unsaturated transport experiments were therefore performed using *Deinococcus radiodurans* cells that were harvested during the log phase and continuously supplied with nutrients during the experiments. Additional experiments were conducted using this bacterium in the stationary phase. Different water saturations were considered in these studies, namely 100 (only stationary phase), 80, and 40%. Results from this study clearly indicated that the physiological state of the bacteria influenced its transport and deposition in sands. Metabolically active bacteria were more hydrophobic and exhibited greater deposition than bacteria in the stationary phase, especially at a water saturation of 40%. The breakthrough curves for active bacteria also had low concentration tailing as a result of cell growth of retained bacteria that were released into the liquid phase. Collected breakthrough curves and deposition profiles were described using a model that simultaneously considers both chemical attachment and physical straining. New concepts and hypotheses were formulated in this model to include biological aspects associated with bacteria growth inside the porous media.

Introduction

Various contaminants have been improperly disposed of or inadvertently released into the vadose zone. Infiltrating water, which serves to recharge to groundwater supplies, may subsequently pass through these contaminated regions and leach contaminants to drinking water supplies. Bioremediation strategies such as bioaugmentation, biostimulation, and natural attenuation have been proposed as cost-effective means to clean up these contaminated sites (1, 2). These techniques rely on the use of metabolically active bacteria

to degrade or immobilize recalcitrant pollutants (3–8). Bioaugmentation involves the introduction of cultured microorganisms that are able to metabolize and grow on the compounds of interest. In biostimulation the subsurface environment is modified by adding limiting nutrients to “stimulate” native bacteria that are capable of degrading contaminants. Natural attenuation uses the existing microbial community and subsurface conditions to contain the spread of contamination and to reduce concentrations.

Bioremediation has many advantages compared with other cleanup methods. For example, since the contamination can be treated *in situ*, the technology does not incur removal and disposal costs and thus post-cleanup costs can be substantially reduced. Although bioremediation holds great promise for dealing with intractable environmental problems, it is important to recognize that much of this promise has yet to be realized. This is due in part to our lack of understanding of microorganism interactions in different hydrologic environments and our inability to efficiently deliver microorganisms from an injection point to a contaminant plume or source zone. The design of efficient bioremediation strategies can be improved by a better understanding of the complex interplay of chemical, biological, and physical factors affecting bacteria transport and deposition.

One of the unresolved problems in bioaugmentation operations is our inability to predict the distribution of the inoculated bacteria throughout the soil profile. This information is needed to ensure adequate contact between specialized bacteria and target compounds. Early adsorption of bacteria can be detrimental to a successful remediation process. In particular, very little is known about transport and deposition of bacteria that are metabolically active. The majority of transport studies have been performed using bacteria cells that were unable to grow and reproduce, or were harvested in the late stationary phase of growth (4, 7, 9, 10).

In practical bioremediation applications, the bacteria cells must be metabolically active and be able to reproduce. In this case, the bacteria must be supplied with nutrients or be able to use components of the liquid or solid phases as a nutrient source. The status of bacteria needs to be considered since the transport behavior of metabolically active and nonactive bacteria cells may exhibit significant differences. Microbiological effects associated with the activity of the cells have typically been neglected in transport studies, but may prove to be significant for many practical bioremediation applications.

Differences in transport and deposition behavior can be caused by bacteria surface properties (6, 8, 11) that will influence interactions with the surfaces of solid soil particles (8). The nature of bacteria cell surfaces is a function of their physiological state (3, 12). It has been reported in the literature that the growth phase influences the cell surface hydrophobicity (13–15) and electrophoretic mobility (16). The hydrophobicity of bacteria surfaces has an important influence on their attachment to a solid matrix (3, 11, 13). Since hydrophobicity also plays a role in the initial adhesion of bacteria to the air–water interface (4, 17, 18), its influence on bacteria transport under unsaturated conditions can also be expected.

Incorporation of microbial processes into transport models has typically proceeded along two separate lines of investigation (19): bacteria transport has commonly been considered to be similar to that of inert colloids (4, 10); or the biodegradation of dissolved contaminants has been

* Corresponding author phone: 0049(2461)618783; fax: 0049(2461)618100; e-mail: g.gargiulo@fz-juelich.de.

† Institute of Chemistry and Dynamics of the Geosphere.

‡ USDA-ARS.

§ University of California.

modeled in the presence of a stationary bacteria that responds to various concentrations of substrates and electron acceptors (20–22). Since changes in metabolic activity may significantly alter the deposition rates of bacteria to solid surfaces, we have investigated how the physiological state of the bacteria impacts their movement through unsaturated systems and how these processes and factors can be mathematically modeled. An existing transport model that simultaneously accounts for attachment/detachment and time- and depth-dependent straining processes (23) has been expanded to consider possible changes due to cellular division and to take into account the more dynamic situations resulting from the metabolic activity of bacteria.

Materials and Methods

Bacteria. *Deinococcus radiodurans* (DSMZ 20539) is a Gram-positive, nonmotile, non-spore-forming, spherical (diameter 1.0–1.5 μm), obligate aerobic bacterium. Bacteria were grown on the agar plates consisting of ATCC Medium 220: CASO AGAR (Merck 105458), peptone from casein (15.0 g), peptone from soy meal (5.0 g), NaCl (5.0 g), agar (15.0 g), and distilled water (1000.0 mL). For column experiments the cells were cultivated at 30 °C in a nutrient broth that was agitated at 130 rpm using a thermostated shaker (Certomax HK BRAUN). The nutrient broth consisted of casein peptone, tryptic digest (10.0 g), yeast extract (5.0 g), glucose (5.0 g), NaCl (5.0 g), and distilled water (1000.0 mL). The bacteria cells were harvested from the nutrient broth during the log phase by gentle centrifugation (10 min, 7100g, 25 °C) and resuspended in fresh media.

More detailed information on the surface characteristics and morphology of *Deinococcus radiodurans* has been previously reported (11). The low degree of hydrophobicity of this bacterium was quantified using the Microbial Adhesion to Hydrocarbon (MATH) approach (24).

Sand. Sterile fused silica sand (Teco-Sil, C-E Minerals Greenville, USA) was used as the porous medium in the column experiments. The median grain size and the coefficient of uniformity of this sand were determined to be 567 μm and 1.87, respectively. The van Genuchten (25) water retention curve and hydraulic conductivity function parameters were determined from multistep outflow data and inverse modeling (26). According to this approach, the porosity was 0.428, the saturated hydraulic conductivity was 0.576 cm min⁻¹, and the empirical parameters α , n , and l were 0.0234 cm⁻¹, 12.13, and 3.617, respectively (11).

Column Experiments. Only stationary phase bacteria could be used in transport experiments conducted at 100% water saturation because these bacteria are obligate aerobes. Both stationary-phase and log-phase bacteria were used in unsaturated transport experiments (80 and 40% water saturation). Description of the setup used in the packed column experiments has been previously reported (11). Only an abbreviated discussion is provided below.

The experimental column was constructed from Plexiglas and was 8 cm in diameter and 22.5 cm long. The air phase in the column was maintained at atmospheric pressure by means of two aeration openings. The column was equipped with tensiometers and pressure transducers near the top, in the middle, and at the bottom of the column to measure the matrix potential and to verify the uniformity of water saturation within the column under steady-state unit gradient (uniform matrix potential with depth) conditions. At the top of the column a sprinkling plate equipped with 80 stainless steel needles was used to evenly distribute the influent over the sand surface at a rate of 165–170 mL/h. The water and the solution were supplied to the sprinkling plate using a piston pump. The bottom was formed by a porous stainless-steel plate covered with a hydrophilic membrane (polyester fabric, mesh size 15 μm). The suction at the bottom of the

column was adjusted to achieve unit gradient by changing the drip point elevation of a hanging water column. Steady-state water flow conditions were kept constant for the remainder of the transport experiment. The total column water content was continuously monitored gravimetrically using a digital balance. The column bottom was connected sequentially with PVC tubes to a conductivity probe (tracer), spectrophotometer, and UV detector (bacteria). Both the bacteria and the tracer outflow concentrations were monitored online.

For full water saturation (100%), the column was completely evacuated using a vacuum pump and subsequently flushed from the top with degassed buffer solution. In experiments conducted at 80% water saturation, water was introduced into the column by slowly pumping upward at a constant rate until a water saturation of approximately 80% was achieved. In contrast, water saturation of 40% was obtained by gradually reducing the inflow rate at the top while at the same time increasing the suction pressure at the bottom until unit gradient conditions were achieved (11). Before initiating the transport experiment with stationary phase cells, the sand pack was equilibrated by flushing it with several pore volumes of phosphate buffer solution (pH = 7 and 10⁻⁴ M). The solution used for the experiment with metabolically active bacteria was composed of peptone from casein (15.0 g), peptone from soy meal (5.0 g), NaCl (5.0 g), and distilled water (1000.0 mL) diluted 1000 times.

The final spatial distribution of retained bacteria was measured following each transport experiment according to the procedure described elsewhere (11). The deposition profile of retained cells per gram of dry sand was determined from measured values of the total organic carbon content (TOC) in the sand. Experimental mass balance was calculated independently for the cells in the effluent and retained cells and normalized by the total number injected into the column.

Theoretical Basis. The HYDRUS-1D code (27) was used to characterize the experimental data collected in this study. The bacteria transport was modeled using a modified form of the convection-dispersion equation, in which 2 kinetic adsorption sites were considered, and first-order kinetic growth was assumed on the solid and liquid phases. The mass balance equation is defined as follows:

$$\frac{\partial \theta C}{\partial t} + \rho_b \frac{\partial s_1}{\partial t} + \rho_b \frac{\partial s_2}{\partial t} = \frac{\partial}{\partial x} \left(\theta D \frac{\partial C}{\partial x} \right) - \frac{\partial q C}{\partial x} + \mu_w \theta C + \mu_s \rho_b (s_1 + s_2) \quad (2)$$

where θ is the volumetric water content; ρ_b [ML⁻³; where M and L denote units of mass and length, respectively] is the soil bulk density; t [T; T denotes units of time] is the time; q [LT⁻¹] is the flow rate; x [L] is the spatial coordinate; D [L²T⁻¹] is the dispersion coefficient; C [N_c L⁻³; where N_c is the number of bacteria cells] is the bacteria concentration in the aqueous phase; s_1 [N_c M⁻¹] and s_2 [N_c M⁻¹] are the solid-phase concentrations associated with sites 1 and 2, respectively; and μ_w [T⁻¹] and μ_s [T⁻¹] are the liquid- and solid-phase growth coefficients, respectively.

Several studies (23, 28) divided sorption sites into two fractions ($s = s_1 + s_2$) and assumed different rates or processes occurring at each sorption site. Bradford et al. (23) assumed that the first fraction of sorption sites, s_1 , represents processes of attachment/detachment and the second fraction, s_2 , represents irreversible straining. The mass balance equation for the solid phase is given as follows when growth on the solid phase is also considered:

$$\rho \frac{\partial s}{\partial t} = \rho \frac{\partial (s_1 + s_2)}{\partial t} = \theta k_a C - k_d \rho_b s_1 + \theta k_{str} \psi_x C + \mu_s \rho_b (s_1 + s_2) \quad (3)$$

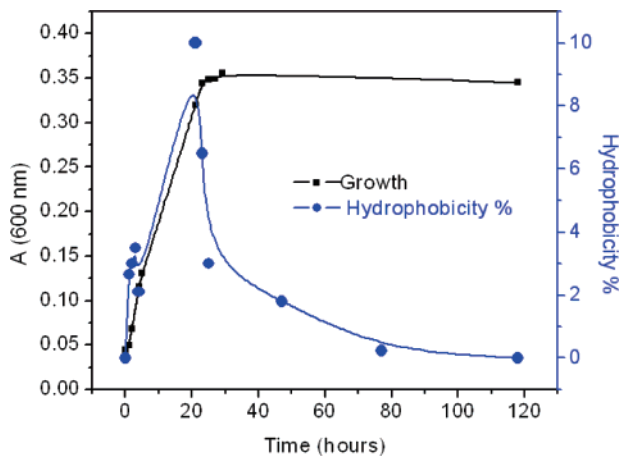


FIGURE 1. *Deinococcus radiodurans* growth curve (left) and hydrophobicity % (right) measured as a function of time.

where k_a [T^{-1}] is the attachment coefficient; k_d [T^{-1}] is the detachment coefficient; k_{str} [T^{-1}] is the straining coefficient; and ψ_t and ψ_x are dimensionless colloid retention functions that account for time- and depth-dependent deposition on site 2, respectively. In this analysis, attachment to the solid phase and the air–water interface can be lumped in the k_a term. Similarly, straining in pores and water films is also considered to be lumped using the k_{str} term.

Bradford et al. (23) hypothesized that the influence of depth-dependent straining processes on colloid retention can be described using the following coefficient:

$$\psi_x = \left(\frac{d_c + x - x_0}{d_c} \right)^{-\beta} \quad (4)$$

where d_c [L] is the median diameter of the sand grains, x_0 [L] is the coordinate of the location where the straining process starts (in this case the surface of the soil profile), and β is an empirical factor controlling the shape of the spatial distribution.

The code allowed us to simultaneously fit the bacteria transport parameters (k_a , k_d , k_{str} , β , μ_l and μ_s) while considering both the breakthrough curve and the retention profile in the nonlinear least-squares optimization routine. To minimize the potential for non-unique parameter fits, we used available experimental information to limit the number of parameters that were considered in these optimizations. Our selection procedure for parameter optimization will be discussed below in the Model Applications section. The mean pore water velocity and dispersivity that were used in simulations reported herein were obtained by fitting the solution of the convective dispersion equation for the tracer breakthrough curve.

Results and Discussion

Growth Curve and Hydrophobicity. Figure 1 shows the growth curve of *Deinococcus radiodurans* obtained by monitoring the cells suspension optical density (OD) and the bacteria surface hydrophobicity (measured using the MATH test) over the course of the bacterial growth curve. The first increase of the OD was detected between 6 and 7 h, with its value increasing from 0.06 to 0.08, indicating the end of the lag phase and the beginning of the log phase (bacteria binary division). After 28–29 h the OD stopped changing. This observation was clear evidence that the log phase was completed and the cells' metabolic activity ended. After about 30 h the bacteria culture entered the stationary phase; i.e., only weak metabolic activity and no increase in the number of bacteria.

TABLE 1. Percentage of Bacteria in the Outflow and Retained in the Column

saturation	log phase			stationary phase	
	outflow	tail	retained	outflow	retained
80%	75%	6%	45%	88%	14%
40%	39%	8%	87%	47%	53%

Inspection of Figure 1 demonstrates that the growth conditions influence the cell surface hydrophobicity of *Deinococcus radiodurans*. The initial hydrophobicity percentage was zero and nearly constant, with values scattered between 0 and 3%, during the lag phase. The hydrophobicity then increased during logarithmic growth, reaching a maximum value of almost 10% at the beginning of the stationary phase. As the stationary phase advanced, the hydrophobicity started to decrease and reached the initial value of 0% after about 100 h. In summary, during a period of high growth rates the bacteria were observed to become more hydrophobic, reaching a maximum value at the end of the log phase and the beginning of stationary phase, whereas lower hydrophobicity was measured during the subsequent phase of nutrient starvation, until it returned to its initial value.

These results are in agreement with other observations reported in the literature that indicate starvation decreased bacteria hydrophobicity and their adhesion to solid surfaces (13–15, 29, 30). Such changes in bacteria hydrophobicity have been attributed to changes in the surface molecular composition during the different life phases of the bacteria. Proteins and polysaccharides are molecules involved in interactions of bacteria cells with the solid interface (31). Since proteins and amino acids are hydrophobic components of extracellular polysaccharide, increased numbers of these molecules cause an increase in the surface bacteria hydrophobicity (8). Moreover, it was observed that bacteria starvation caused a decrease in the concentration of surface proteins (32). The bacteria hydrophobicity observed during the growth stage may be attributed to an initial increase in the amount of proteins on the bacteria surface during the log phase. A subsequent decrease in hydrophobicity may thus be caused by the decrease in the surface proteins during cell starvation.

Gargiulo et al. (11) reported on differences in shape and morphology of the log and stationary phase *Deinococcus radiodurans*. Log phase *Deinococcus radiodurans* tend to form pairs and tetrads of around 2–4 μm in diameter when grown in nutrient both. Conversely, stationary phase *Deinococcus radiodurans* occurred primarily as single cells. Differences in the size of log and stationary phase *Deinococcus radiodurans* likely occurred as a result of differences in cell surface hydrophobicity (Figure 1). Colloid stability and aggregation is reported to be sensitive to the surface hydrophobicity (33, 34); i.e., hydrophobic colloids are less stable than hydrophilic colloids.

Decreasing hydrophobicity of soil bacteria during starvation has been recognized to be a result of a survival strategy (14). Under optimal growth (nutrient) conditions, it is beneficial for soil bacteria cells to be more hydrophobic and to firmly attach to solid surfaces and to each other. On the other hand, under unfavorable nutrient conditions, the hydrophilic microorganisms are smaller (less aggregation) and may more easily detach themselves from solid surfaces and be transported in the liquid phase to a new location in the environment that is richer in nutrients.

Transport and Deposition. Table 1 provides mass balance information for the bacteria transport experiments. Very good mass balance was obtained for the stationary phase bacteria (100–102%), and provides a high degree of confidence in our experimental procedures. Conversely, it was not possible

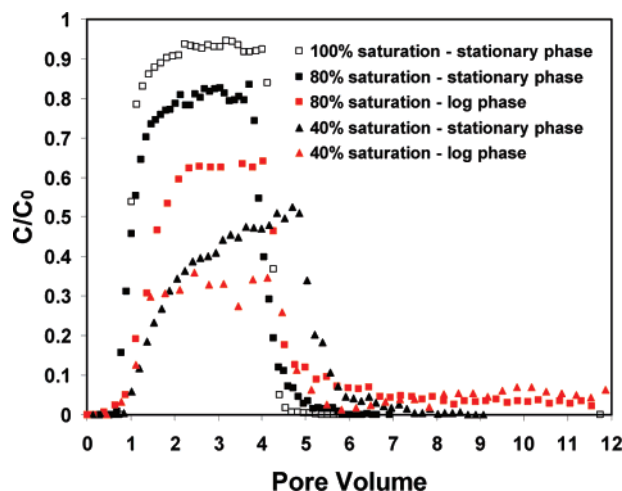


FIGURE 2. Comparison of breakthrough curves for *Deinococcus radiodurans* at different saturations (100, 80, and 40%) and in different growth phases (stationary and log phases). Only stationary-phase bacteria could be used in transport experiments conducted at 100% water saturation because the bacteria are obligate aerobes. Here the relative concentration, C/C_0 where C_0 is the influent bacteria concentration, is plotted as a function of pore volume.

to close the mass balance for bacteria with cells in the log phase because of binary division that occurred during the experiment. The total number of cells recovered after the experiment exceeded by about 30% the total number of cells injected in the soil column.

Figure 2 compares the breakthrough curves (here relative concentrations, C/C_0 , are plotted as a function of pore volume) for *Deinococcus radiodurans* in the stationary and/or growing (log) phases at saturations of 100, 80, and 40%. Only stationary phase bacteria could be used in transport experiments conducted at 100% water saturation because these bacteria are obligate aerobes. The breakthrough curves show significant differences in the maximum relative concentrations, in the curve shapes, and in the concentration trailing between bacteria in the stationary and metabolically active phases at the various saturations.

For a given saturation (80 and 40%), lower effluent concentrations were observed for the metabolically active bacteria than for the stationary phase cells (Figure 2).

Although breakthrough curves at 80% saturation reached a plateau for bacteria in both stationary and growth phases, their maximum relative concentrations were different. The maximum relative concentration for the metabolically active cells in the log phase ($C/C_0 = 0.63$) was lower than for cells in the stationary phase ($C/C_0 = 0.83$). At 40% saturation, the maximum relative concentrations in the outflow were also significantly different for the stationary ($C/C_0 = 0.5$) and log-phase ($C/C_0 = 0.3$) bacteria. This enhanced retention for the metabolically active bacteria may be attributed to more cell-cell interactions as a result of differences in hydrophobicity (Figure 1) and larger cell/aggregate (1.0 compared to 2–4 μm for stationary and log-phase cells, respectively) sizes. Both attachment and straining are predicted to increase with increasing cell/aggregate size (23, 35).

For a given growth phase (stationary or growth), lower effluent concentrations were also observed for decreasing water saturation (Figure 2). The maximum relative concentration for the stationary phase cells at 100, 80, and 40% water saturation was 0.92, 0.83, and 0.5, respectively. The maximum relative concentration for active cells at 80 and 40% water saturation was 0.63 and 0.3, respectively. Increased retention with decreasing water saturation has been observed by other researchers (4, 9–11, 18, 36), and has been attributed to attachment at the air–water interface (4, 9, 10), film straining (18), and more recently to straining (11, 36).

The overall shape of breakthrough curves shown in Figure 2 for bacteria in different phases was different as well. Bacteria in the resting phase at 40% water saturation clearly exhibit a decreasing rate of deposition with time. In contrast, in the metabolically active phase the deposition of successive cells on each other is not prevented. Metabolically active bacteria cells that are deposited on the sand surface apparently do not inhibit the retention of additional bacteria because the active cells have stronger cell–cell interactions. The enhanced cell–cell interactions for metabolically active bacteria could be explained with the increased cell hydrophobicity during the experiment (Figure 1) (29) and the higher number and extension of surface macromolecules compared to bacteria in the resting mode (30, 32). This could have resulted in enhanced polymer bridging.

Contrary to the stationary state, the breakthrough curve of the log-phase bacteria showed pronounced tailing, with the outflow concentrations not reaching zero values even after 15 pore volumes (Figures 2, 3A, and 4A). This phe-

TABLE 2. Model Parameters for *Deinococcus radiodurans* in Different Growth Phases and at Different Saturations

	saturation					
	100%		80%		40%	
	value	S.E.coeff.	value	S.E.coeff.	value	S.E.coeff.
<i>Deinococcus radiodurans</i> (stationary phase)						
k_a (min^{-1})	4.54×10^{-5}	1.69×10^{-4}	3.38×10^{-3}	5.27×10^{-4}	9.77×10^{-2}	2.15×10^{-2}
k_d (min^{-1})	2.27×10^{-3}	2.13×10^{-2}	2.78×10^{-2}	5.33×10^{-3}	7.70×10^{-2}	1.79×10^{-2}
k_{str} (min^{-1})	5.12×10^{-3}	1.27×10^{-3}	1.73×10^{-2}	4.72×10^{-4}	7.77×10^{-2}	4.34×10^{-3}
β	0.432		0.432		0.432	
R^2	0.994		0.996		0.928	
R^2 (btc ^a)	0.994		0.998		0.931	
R^2 (rp ^a)	0.980		0.954		0.896	
<i>Deinococcus radiodurans</i> (log phase)						
k_a (min^{-1})	N/A	N/A	4.29×10^{-3}	4.39×10^{-4}	1.08×10^{-2}	1.35×10^{-3}
k_d (min^{-1})	N/A	N/A	6.84×10^{-4}	1.57×10^{-4}	1.64×10^{-3}	3.81×10^{-4}
k_{str} (min^{-1})	N/A	N/A	1.72×10^{-2}	2.73×10^{-3}	9.33×10^{-2}	6.30×10^{-3}
μ_s (min^{-1})	N/A	N/A	4.87×10^{-4}	5.20×10^{-5}	1.45×10^{-4}	3.05×10^{-5}
β	N/A	N/A	0.432		0.432	
R^2	N/A	N/A	0.957		0.956	
R^2 (btc ^a)	N/A	N/A	0.957		0.865	
R^2 (rp ^a)	N/A	N/A	0.959		0.984	

^a btc = breakthrough curve; rp = retention profile.

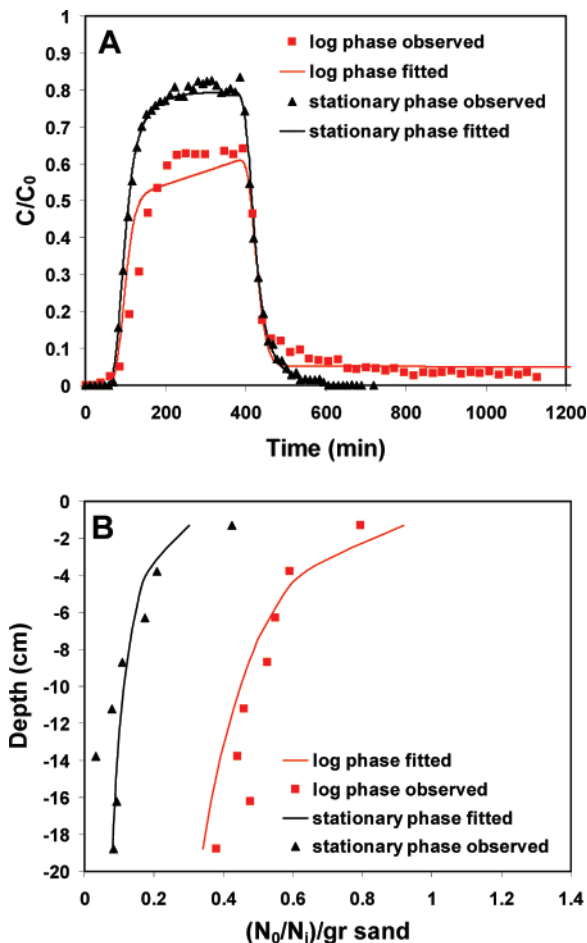


FIGURE 3. Measured and fitted breakthrough curves (A) and retention profiles (B) for *Deinococcus radiodurans* for cells in the stationary (100 and 80% water saturation) and log (80% water saturation) phases. In A the relative effluent concentration is plotted as a function of time. In B the normalized concentration (number of bacteria recovered in the sand, N_c , is divided by the number in a unit volume of the input bacterial suspension, N_i) per gram of dry sand and these are plotted as a function of the distance from the column inlet.

nomenon was attributed to cell growth. We hypothesize that the pronounced tailing was due to continuous bacteria multiplication in the solution and due to the mechanism called “cell division mediated transport” (37, 38). During cell division mediated transport the mother cells deposit on the mineral surface, grow, divide, and finally release the daughter cells into the aqueous phase.

The retention profiles at all saturations and for both active and nonactive cells were not exponential with depth as predicted by classical filtration theory (see values of β in Table 2). The deposition profiles exhibited invariably greater retention in the section adjacent to the column inlet (Figures 3B and 4B). This incongruence with CFT has been reported by other researchers under both saturated (5, 23, 39–44) and unsaturated (10, 11, 36) conditions. The log-phase bacteria showed a more pronounced presence of bacteria at the column inlet than stationary bacteria at both saturations (80 and 40%). The log phase bacteria likely had enhanced cell–cell interactions and straining at the column inlet presumably due to the presence of more extensive protein molecules on the bacteria surface that caused “polymer bridging” and due to their larger cell/aggregate sizes. The relative number of bacteria present throughout the soil column is also higher in the case of log-phase cells compared with the stationary-phase cells. This observation can be attributed to enhanced

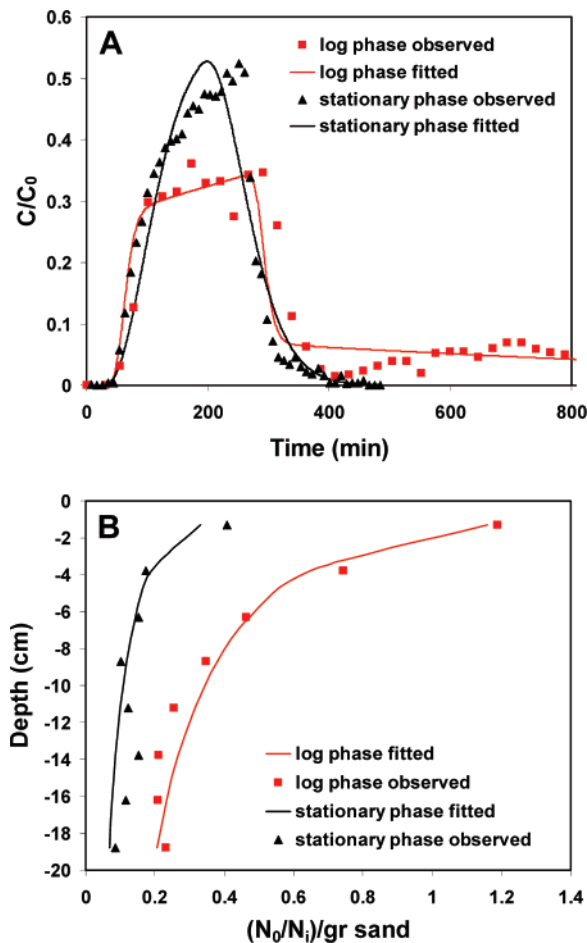


FIGURE 4. Measured and fitted breakthrough curves (A) and retention profiles (B) for *Deinococcus radiodurans* at 40% saturation for cells in stationary and log phases. In A the relative effluent concentration is plotted as a function of time. In B the normalized concentrations per gram of dry sand are plotted as a function of the distance from the column inlet.

attachment due to different surface characteristics of the metabolically active bacteria compared with the resting mode cells. In particular, proteins on the surface of active bacteria cells enhance the hydrophobicity and attachment along the soil packing.

Model Application. For stationary phase transport experiments the values of μ_w and μ_s were considered equal to zero because no growth occurred, and attachment (k_a and k_d) and straining (k_{str}) model parameters were fit to breakthrough curves and deposition profiles. Model fits were more complicated for log phase transport experiments because growth also occurred in the liquid and solid phases. In this case, attachment (k_a and k_d), straining (k_{str}), and growth (μ_w and μ_s) model parameters were fit to breakthrough curves and deposition profiles. To minimize the number of fitting parameters that were optimized, the value of β in eq 4 was set equal 0.432 based on previously published findings (23) when significant straining occurred. According to this modeling approach the influence of attachment and straining processes dominate different regions of the deposition profile (23); i.e., straining dominates near the sand surface and attachment dominates at greater transport distance.

Very good agreement was obtained between the observed and simulated data for the metabolically active and resting phases of the bacteria at both saturations (Figures 3A and B, 4A and B). Values of optimized parameters are summarized in Table 2. The attachment, k_a , detachment, k_d , and straining, k_{str} , coefficients increased as the saturation decreased (Table

2) for both the resting mode cells and the log-phase bacteria. The attachment coefficient, which lumps attachment to the solid phase and the air–water interface, slightly increased as saturation decreased, probably due to the enhanced attachment to the air–water interface as the air–water interfacial area increased (11). Increasing values of k_a with decreasing saturation, suggests that attachment to the air–water interface is approaching linear equilibrium conditions (45). Straining has been hypothesized to increase with decreasing water saturation because more of the water flux flows through small straining sites at lower saturations (11).

For a given water saturation, the value of k_{str} was very similar for stationary- and log-phase cells. This finding suggests that straining is not much affected by the growth stage for these bacteria. In contrast, parameter values for k_a and k_d were very dependent on the growth stage of the cells. In particular, the values of k_d were significantly lower for metabolically active cells. This observation indicates that stronger cell–cell interactions occurred for attached bacteria under active growth conditions. It is well-known that many bacteria are capable of forming a biofilm. Under certain conditions the bacteria cells communicate with each other by means of a process called quorum sensing and detect when they are assembled in large numbers as opposed to when they are essentially alone (46). According to this theory, bacteria in favorable growing conditions secrete and sense small signalling molecules to communicate and to promote biofilm formation. The metabolically active cells are not likely to reject each other and the deposition of one cell should not inhibit the deposition of the next cell. The cells try to get as close as possible to each other to form a more resistant structure. This effect may be further enhanced by increased hydrophobicity of metabolically active bacteria and the associated higher number and extension of proteins on the surface of these bacteria.

Mass balance information after recovery of the concentration plateau region of the breakthrough curve (before significant detachment occurred) also supports this enhanced cell–cell interaction hypothesis. Attachment for active and stationary cells accounted for 59.1 and 14.9% of the retained cell mass at a water saturation of 80%, respectively. Similarly, attachment for active and stationary cells accounted for 35.2 and 16.6% of the retained cell mass at a water saturation of 40%, respectively. Hence, increased deposition of log-phase compared to stationary-phase bacteria are attributed primarily to attachment. Straining was always the dominant mechanism of retention (>83.4%) for the stationary-phase bacteria. For log-phase cells, however, straining accounted for 40.9 and 64.8% of the retained cells at a water saturation of 80 and 40%, respectively.

The plateau region of the breakthrough curves shown in Figure 2 did not change much with time for the log-phase bacteria transport experiments, and suggests that μ_1 was low and only accounted for a small fraction of C_0 . Preliminary model fits to this data also indicated that the value of μ_1 was very low ($<0.46 \times 10^{-4} \text{ min}^{-1}$), and that the value of μ_s was significantly higher (1 order of magnitude) than that of μ_1 . This result indicates that the deposited cells have a higher division rate compared with the cell in the bulk solution. To minimize the potential for non-unique parameter fits, we therefore set the value of μ_1 to zero in subsequent simulations with log-phase cells. Table 2 provides values of μ_s when μ_1 was set equal to zero. The tailing of the bacteria outflow concentrations could be well described by this model formation at both saturations (80% and 40%) (Figures 3A and 4A). These observations support our hypotheses that deposited bacteria are particularly active in biofilm formation under favorable growth conditions and that the observed tailing in the breakthrough curves was primarily due to release of the daughter cells into the aqueous solution from attached

mother cells (cell-division mediated transport).

Results from this study clearly indicate that the physiological state of the bacteria will influence its transport and deposition in soils producing a more dynamic system and resulting in different effluent breakthrough curves and deposition profiles for metabolically active bacteria. Additional studies are warranted to better understand bioremediation processes and to design more effective technologies. For example, further transport studies with different bacteria strains during their active states, and to better deduce mutual bacterial interactions, are desirable. The coupled influence of various pollutants, nutrients, substrates, and electron acceptors on the physiological state of the bacteria and their transport potential are topics of future studies.

Acknowledgments

G.G. thanks the Forschungszentrum Juelich, Germany, for the financial support of this project.

Literature Cited

- Mishra, S.; Jeevan, J.; Ramesh, C. K.; Banwari, L. In situ bioremediation potential of an oily sludge-degrading bacterial consortium. *Curr. Microbiol.* **2001**, *43*, 328–335.
- Vidali, M. Bioremediation. An overview. *Pure Appl. Chem.* **2001**, *73* (7), 1163–1172.
- Grasso, D.; Smets, B. F.; Strevett, K. A.; Machinist, B. D.; Van Oss, C. J.; Giese, R. F.; Wu, W. Impact of physiological state on surface thermodynamics and adhesion of *Pseudomonas aeruginosa*. *Environ. Sci. Technol.* **1996**, *30*, 3604–3608.
- Schaefer, A.; Ustohal, P.; Harms, H.; Stauffer, F.; Dracos, T.; Zehnder, A. J. B. Transport of bacteria in unsaturated porous media. *J. Contam. Hydrol.* **1998**, *33*, 149–169.
- Bolster, C. H.; Mills, A. L.; Hornberger, G. M.; Herman, J. S. Effect of surface coatings, grain size, and ionic strength on the maximum attainable coverage of bacteria on sand surfaces. *J. Contam. Hydrol.* **2001**, *50*, 287–305.
- Mehmannavz, R.; Prasher, S. O.; Ahmad, D. Cell-surface properties of rhizobial strains isolated from soils contaminated with hydrocarbons: hydrophobicity and adhesion to sandy soil. *Process Biochem.* **2001**, *36* (7), 683–688.
- Tufenkji, N.; Redman, J. A.; Elimelech, M. Interpreting Deposition Patterns of Microbial Particles in Laboratory-Scale Column Experiments. *Environ. Sci. Technol.* **2001**, *37*, 616–623.
- Sanin, S. L. Effect of Surface Properties and Flow Regime on the Transport of Bacteria in Groundwater: An Experimental Approach. *Turkish J. Eng. Environ. Sci.* **2004**, *28*, 317–324.
- Wan, J.; Wilson, J. L.; Kieft, T. L. Influence of the gas water interface on transport of microorganisms through unsaturated porous media. *Appl. Environ. Microbiol.* **1994**, *60*, 509–516.
- Jewett, D. G.; Logan, B. E.; Arnold, R. G.; Bales, R. C. Transport of *Pseudomonas fluorescens* strain P17 through quartz sand columns as a function of water content. *J. Contam. Hydrol.* **1998**, *36*, 73–89.
- Gargiulo, G.; Bradford, S.; Šimůnek, J.; Ustohal, P.; Vereecken, H.; Klumpp, E. Bacteria transport and deposition under unsaturated conditions: the role of water content and bacteria surface hydrophobicity. *Appl. Environ. Microbiol.* Submitted.
- Sandrin, S. K.; Jordan, F. L.; Maier, R. M.; Brusseau, M. L. Biodegradation during contaminant transport in porous media: Impact of microbial lag and bacterial cell growth. *J. Contam. Hydrol.* **2001**, *50* (3–4), 225–242.
- Van Loosdrecht, M. C. M.; Lyklema, J.; Norde, W.; Schraa, G.; Zehnder, A. J. B. The role of bacterial cell wall hydrophobicity in cell attachment. *Appl. Environ. Microbiol.* **1987**, *53*, 1893–1897.
- Van Loosdrecht, M. C. M.; Lyklema, J.; Norde, W.; Schraa, G.; Zehnder, A. J. B. Electrophoretic mobility and hydrophobicity as a measure to predict the initial steps of bacterial adhesion. *Appl. Environ. Microbiol.* **1987**, *53*, 1898–1901.
- Sanin, S. L.; Sanin, F. D.; Bryers, J. D. Effect of starvation on the adhesive properties of xenobiotic degrading bacteria. *Process Biochem.* **2003**, *38*, 909–914.
- Gilbert, P.; Evans, D. J.; Evans, E.; Duguid, I. G.; Brown, M. R. W. Surface characteristics and adhesion of *Escherichia coli* and *Staphylococcus epidermidis*. *J. Appl. Bacteriol.* **1991**, *71*, 72–77.
- Dahlback, B.; Hermansson, M.; Kjelleberg, S.; Norrans, B. The hydrophobicity of bacteria-an important factor in their initial

- adhesion at the air-water interface. *Arch. Microbiol.* **1981**, *128* (3), 267–270.
- (18) Wan, J.; Tokunaga, T. K. Film straining of colloids in unsaturated porous media: Conceptual model and experimental testing. *Environ. Sci. Technol.* **1997**, *31*, 2413–2420.
- (19) Murphy, E. M.; Ginn, T. R. Modeling microbial processes in porous media. *Hydrogeol. J.* **2000**, *8*, 142–158.
- (20) Broholm, K.; Christensen, T. H.; Jensen, B. K. Modelling TCE degradation by a mixed culture of methane-oxidizing bacteria. *Water Res.* **1992**, *26* (9), 1177–1185.
- (21) Horstad, I.; Larter, S. R.; Mills, N. Quantitative model of biological petroleum degradation within the Brent Group reservoir in the Gullfaks Field, Norwegian North Sea. *Org. Geochem.* **1992**, *19* (1–3), 107–117.
- (22) Battistelli, A. Modeling Biodegradation of organic contaminants under multiphase conditions with TMVOCBio. *Vadose Zone J.* **2004**, *3*, 875–883.
- (23) Bradford, S. A.; Šimůnek, J.; Bettahar, M.; Van Genuchten, M. Th.; Yates S. R. Modeling colloid attachment, straining and exclusion in saturated porous media. *Environ. Sci. Technol.* **2003**, *37*, 2242–2250.
- (24) Rosenberg, M.; Rosenberg, E.; Gutnick, D. Bacterial adherence to hydrocarbons. In *Microbial Adhesion to Surfaces*; Berkeley, R. C. W., Lynch, J. M., Melling, J., Rutter, P. R., Vincent, B., Eds.; Soc Chem. Ind.: London, U.K., 1980; pp 541–542.
- (25) Van Genuchten, M. Th. A closed-form equation for predicting the hydraulic conductivity of unsaturated soils. *Soil Sci. Soc. Am. J.* **1980**, *44*, 892–898.
- (26) Hopmans, J. W.; Šimůnek, J.; Romano, N.; Durner, W. Inverse modeling of transient water flow. In *Methods of Soil Analysis, Part 1, Physical Methods*, 3rd ed.; Dane, J. H., Topp, G. C., Eds.; Soil Science Society of America; Madison, WI, 2002; pp 963–1008.
- (27) Šimůnek, J.; Van Genuchten M. Th.; Šejna, M. The HYDRUS-1D software package for simulating the one-dimensional movement of water, heat, and multiple solutes in variably-saturated media. Version 3.0, HYDRUS Software Series 1; Department of Environmental Sciences, University of California Riverside, Riverside, CA, 2005; 270 pp.
- (28) Schijven, J. F.; Šimůnek, J. Kinetic modeling of virus transport at the field scale. *J. Contam. Hydrol.* **2002**, *55*, 113–135.
- (29) Fattom, A.; Shilo, M. Hydrophobicity as an adhesion mechanism of benthic cyanobacteria. *Appl. Environ. Microbiol.* **1984**, *47*, 135–143.
- (30) Kjelleberg S.; Hermansson M. Starvation-induced effects on bacterial surface characteristics. *Appl. Environ. Microbiol.* **1984**, *48* (3), 497–503.
- (31) Thomas, D.; Surdin-Kerjan, Y. Metabolism of sulfur amino acids in *Saccharomyces cerevisiae*. *Microbiol. Mol. Biol. Rev.* **1997**, *61*, 503–532.
- (32) Castellanos, T.; Ascencio, F.; Bashan, Y. Starvation-induced changes in the cell surface of *Azospirillum lipoferum*. *FEMS Microbiol. Ecol.* **2000**, *33*, 1–9.
- (33) Crist, J. T.; Zevi, Y.; McCarthy, J. F.; Throop, J. A.; Steenhuis, T. S. Transport and retention mechanisms of colloids in partially saturated porous media. *Vadose Zone J.* **2005**, *4*, 184–195.
- (34) Breiner, J. M.; Anderson, M. A.; Tom, H. W. K.; Graham, R. C. Properties of surface-modified colloidal particles. *Clays Clay Min.* **2006**, *54*, 12–24.
- (35) Tufenkji, N.; Elimelech, M. Correlation equation for predicting single-collector efficiency in physicochemical filtration in saturated porous media. *Environ. Sci. Technol.* **2004**, *38*, 529–536.
- (36) Gargiulo G.; Bradford S.; Šimůnek, J.; Ustohal P.; Vereecken H.; Klumpp E. Bacteria transport and deposition under unsaturated conditions: The role of the matrix grain size and the bacteria surface protein. *J. Contam. Hydrol.* **2007** In press.
- (37) Sharma, P. K.; McInerney M. J.; Knapp R. M. In situ growth and activity and modes of penetration of *Escherichia coli* in unconsolidated porous materials. *Appl. Environ Microbiol.* **1993**, *59*, 3686–3694.
- (38) Ginn, T. R.; Wood, B. D.; Nelson, K. E.; Scheibe, T. D.; Murphy, E. M.; Clement, T. P. Processes in microbial transport in the natural subsurface. *Adv. Water Resour.* **2002**, *25*, 1017–1042.
- (39) DeFlaun, M. F.; Murray, C. J.; Holben, W.; Scheibe, T.; Mills, A.; Ginn, T.; Griffin, T.; Majer, E.; Wilson, J. L. Preliminary observations on bacterial transport in a coastal plan aquifer. *FEMS Microbiol. Rev.* **1997**, *20*, 473–487.
- (40) Bradford, S. A.; Yates S. R.; Bettahar M.; Šimůnek J. Physical factors affecting the transport and fate of colloids in saturated porous media. *Water Resour. Res.* **2002**, *38* (12), 1327; doi: 10.1029/2002WR001340.
- (41) Bradford, S. A.; Šimůnek, J.; Bettahar, M.; Tadassa, Y. F.; Van Genuchten, M. Th.; Yates S. R. Straining of colloids at textural interfaces. *Water Resour. Res.* **2005**, *41*, W10404; doi: 10.1029/2004WR003675.
- (42) Bradford, S. A.; Šimůnek, J.; Bettahar, M.; Van Genuchten, M. Th.; Yates, S. R. Significance of straining in colloid deposition: evidence and implications. *Water Resour. Res.* **2006**, *42*, W12S15; doi:10.1029/2005WR004791.
- (43) Tufenkji, N.; Miller, G. F.; Ryan, J. N.; Harvey, R. W.; Elimelech, M. Transport of *Cryptosporidium* oocysts in porous media: Role of straining and physicochemical filtration. *Environ. Sci. Technol.* **2004**, *38*, 5932–5938.
- (44) Johnson, W. P., Tong, M.; Li, X. Colloid deposition in environmental porous media: Deviation from existing theory is the norm, not the exception. *EOS* **2005**, *86* (18), 179–180.
- (45) Van Genuchten, M. Th.; Davidson, J. M.; Wierenga, P. J. An evaluation of kinetic and equilibrium equations for the prediction of pesticide movement through porous media. *Soil Sci. Soc. Am. J.* **1974**, *38*, 29–35.
- (46) Parsek M. R.; Greenberg P. Acyl-homoserin lactone quorum sensing in Gram-negative bacteria: A signaling mechanism involved in associations with higher organisms. *Colloquium: Proc. Nat. Acad. Sci.* **2000**, *97* (16), 8789–8793.

Received for review December 1, 2006. Accepted December 12, 2006.

ES062854A